Published in final edited form as:
Nat Immunol. 2013 June ; 14(6): 554–563. doi:10.1038/ni.2586.

Mast cell maturation is driven via a group III phospholipase A_2-prostaglandin D_2–DP1 receptor paracrine axis

Yoshitaka Taketomi[1,2], **Noriko Ueno**[1], **Takumi Kojima**[1], **Hiroyasu Sato**[1,2], **Remi Murase**[1,2], **Kei Yamamoto**[1], **Satoshi Tanaka**[3], **Mariko Sakanaka**[4], **Masanori Nakamura**[5], **Yasumasa Nishito**[6], **Momoko Kawana**[2], **Naotomo Kambe**[7], **Kazutaka Ikeda**[8], **Ryo Taguchi**[9], **Satoshi Nakamizo**[10], **Kenji Kabashima**[10], **Michael H. Gelb**[11], **Makoto Arita**[12], **Takehiko Yokomizo**[13], **Motonao Nakamura**[14], **Kikuko Watanabe**[15], **Hiroyuki Hirai**[16], **Masataka Nakamura**[17], **Yoshimichi Okayama**[18], **Chisei Ra**[18], **Kosuke Aritake**[19], **Yoshihiro Urade**[19], **Kazushi Morimoto**[20], **Yukihiko Sugimoto**[20], **Takao Shimizu**[14], **Shuh Narumiya**[21], **Shuntaro Hara**[2], and **Makoto Murakami**[1]

[1]Lipid Metabolism Project, Tokyo Metropolitan Institute of Medical Science, Tokyo, Japan

[2]School of Pharmacy, Showa University, Tokyo, Japan

[3]Department of Immunobiology, Okayama University Graduate School of Medicine, Dentistry and Pharmaceutical Sciences, Okayama, Japan

[4]School of Pharmacy and Pharmaceutical Sciences, Mukogawa Women's University, Hyogo, Japan

[5]School of Dentistry, Showa University, Tokyo, Japan

[6]Core Technology and Research Center, Tokyo Metropolitan Institute of Medical Science, Tokyo, Japan

[7]Department of Dermatology, Chiba University Graduate School of Medicine, Chiba, Japan

[8]Institute for Advanced Biosciences, Keio University, Yamagata, Japan

[9]College of Life and Health Sciences, Chubu University, Aichi, Japan

[10]Department of Dermatology, Kyoto University Graduate School of Medicine, Kyoto, Japan

[11]Departments of Chemistry and Biochemistry, University of Washington, Washington, USA

Correspondence should be addressed to M.M. (murakami-mk@igakuken.or.jp).

Accession code. Gene Expression Ominibus: GSE44980 (microarray data).

Note: Supplementary information is available in the online version of the paper.

AUTHOR CONTRIBUTIONS

Y.T. performed experiments and together with M.M. conceived and designed the study, interpreted the findings and wrote the manuscript; N.U., T.K., M.K., R.M. and H.S. performed experiments; S.T., M.S., Masanori Nakamura, Y.N., K.I., K.M., Satoshi Nakamizo, K.K., Y.O. and C.R. helped perform some experiments; K.Y., N.K., R.T., M.H.G. M.A., T.Y., Masataka Nakamura, K.W., H.H., Motonao Nakamura, K.A., Y.U., Y.S., T.S., Shu Narumiya and S.H. contributed to experimental designs.

COMPETING FINANCIAL INTERESTS

The authors declare no competing financial interests.

[12]Graduate School of Pharmaceutical Sciences, The University of Tokyo, Tokyo, Japan

[13]Department of Biochemistry, Juntendo University School of Medicine, Tokyo, Japan

[14]Faculty of Medicine, The University of Tokyo, Tokyo, Japan

[15]Department of Nutrition, Koshien University, Hyogo, Japan

[16]Department of Advanced Medicine and Development, Bio Medical Laboratories, Saitama, Japan

[17]Human Gene Sciences Center, Tokyo Medical and Dental University, Tokyo, Japan

[18]Division of Molecular Cell Immunology and Allergology, Advanced Medical Research Center, Nihon University Graduate School of Medical Science, Tokyo, Japan

[19]Department of Molecular Bihavioral Biology, Osaka Bioscience Institute, Osaka, Japan

[20]Department of Pharmaceutical Biochemistry, Graduate School of Medicine and Pharmaceutical Sciences, Kumamoto University, Kumamoto, Japan

[21]Department of Pharmacology, Kyoto University Graduate School of Medicine, Kyoto, Japan

Abstract

Microenvironment-based alterations in phenotypes of mast cells influence the susceptibility to anaphylaxis, yet the mechanisms underlying proper maturation of mast cells toward an anaphylaxis-sensitive phenotype are incompletely understood. Here we report that PLA2G3, a mammalian homolog of anaphylactic bee venom phospholipase A_2, regulates this process. PLA2G3 secreted from mast cells is coupled with fibroblastic lipocalin-type PGD_2 synthase (L-PGDS) to provide PGD_2, which facilitates mast-cell maturation via PGD_2 receptor DP1. Mice lacking PLA2G3, L-PGDS or DP1, mast cell–deficient mice reconstituted with PLA2G3-null or DP1-null mast cells, or mast cells cultured with L-PGDS–ablated fibroblasts exhibited impaired maturation and anaphylaxis of mast cells. Thus, we describe a lipid-driven PLA2G3–L-PGDS–DP1 loop that drives mast cell maturation.

Anaphylaxis is a serious immediate allergic reaction that involves the activation of mast cells. Cross-linking of the high-affinity IgE receptor FcεRI on mast cells with IgE and antigen initiates signals leading to the release of allergic mediators that induce immediate hypersensitivity[1]. Anaphylaxis is triggered by allergens (for example, insect venom, food and medication) and damages multiple organs including the respiratory and circulatory systems, often leading to life-threatening episodes.

Environmentally induced alterations in phenotypes of mast cells could be one factor that influences the severity of anaphylaxis. Current evidence has established the essential role of stem cell factor (SCF) and its receptor c-Kit (CD117) for development of mast cells[2]. However, the SCF–c-Kit system alone is insufficient to drive the maturation of mast cells fully, as culture of immature mast cells with fibroblasts, but not with SCF alone, can induce differentiation into mature mast cells[2]. Although several cytokines, chemokines and adhesion molecules have supporting roles in tissue-specific homing, growth or

differentiation of mast cells[3–7], precise mechanisms underlying mast cell–fibroblast communication leading to optimal maturation of mast cells still remain elusive.

Lipid mediators, such as prostaglandins, leukotrienes and lysophospholipids, have important roles in various biological processes, including allergy[8–15]. A given lipid mediator (for example, PGD_2) aggravates, suppresses or resolves allergic responses[11–13], and this functional variability may depend on the use of distinct biosynthetic enzyme and/or receptor subtypes in different cells. Eicosanoid biosynthesis is initiated by release of arachidonic acid from phospholipids by phospholipase A_2 (PLA_2) enzymes[16]. PLA2G4A (cytosolic PLA_2; $cPLA_2\alpha$) has an essential role in the generation of eicosanoids in various cells, and its deletion results in diminished airway hypersensitivity[17]. By contrast, the role of secreted PLA_2 ($sPLA_2$) enzymes is still a subject of debate. Although the lower asthmatic responses in mice lacking two classical $sPLA_2$ enzymes (PLA2G5 and PLA2G10) have revealed their contribution to asthma[18,19], the mechanisms underlying the actions of these enzymes remain poorly understood.

A major bee venom component responsible for anaphylaxis is an atypical form of $sPLA_2$ called BV-PLA_2[20,21]. The mammalian genome encodes group III $sPLA_2$ (PLA2G3), which is the sole homolog of BV-PLA_2[16,22–26]. Here we provide evidence that PLA2G3 is a major mast cell granule-associated $sPLA_2$ that facilitates the maturation of mast cells by driving a previously unrecognized lipid mediator circuit. PLA2G3 released from mast cells is coupled with fibroblast lipocalin-type PGD synthase (L-PGDS) to provide PGD_2, which then acts on type-1 PGD receptor, DP1, induced on mast cells to promote their maturation.

RESULTS

PLA2G3 is expressed in mast cells and induces their activation

When injected intradermally into the mouse ear pinnas, BV-PLA_2 or human PLA2G3 alone induced a similar, dose-dependent vascular leak and augmented passive cutaneous anaphylaxis (PCA) induced by IgE and antigen in $Kit^{+/+}$ mice but not in mast cell–deficient $Kit^{W\text{-}sh/W\text{-}sh}$ mice, in which the SCF receptor c-Kit has a substitution (Fig. 1a,b). The edema induced by PLA2G3 was accompanied by ultrastructural degranulation of dermal mast cells (Fig. 1c). PLA2G3 induced the release of histamine (Fig. 1d), but not of lactate dehydrogenase (Supplementary Fig. 1a), from mouse peritoneal mast cells (pMCs) in a Ca^{2+}-dependent manner, indicating that PLA2G3 elicits degranulation, not cell lysis.

Immunohistochemistry analysis revealed that PLA2G3 localized with toluidine $blue^+$ dermal mast cells in wild-type mice but not in $Pla2g3^{-/-}$ mice[22] (Fig. 1e). Punctate staining in resting mast cells and sparse staining in degranulated mast cells suggest that PLA2G3 is released upon degranulation (Fig. 1e,f). In bone marrow–derived cell populations, *Pla2g3* mRNA was more highly enriched in IL-3–driven bone marrow–derived mast cells (BMMCs) and thymic stromal lymphopoietin (TSLP)-driven bone marrow–derived basophils (BM basophils) than in GM-CSF–driven bone marrow–derived dendritic cells (BMDCs) and M-CSF–driven bone marrow–derived macrophages (BMDMs), and was undetectable in Swiss 3T3 fibroblasts (Fig. 1g and Supplementary Fig. 1b). Of the mRNAs encoding $sPLA_2$ isoforms, *Pla2g3* mRNA was expressed most abundantly in BMMCs,

followed by *Pla2g5* and *Pla2g2e*, whereas mRNAs encoding the other $sPLA_2$ isoforms were undetectable, and SCF-fibroblast–driven maturation of these cells toward connective tissue mast cells (CTMCs) did not affect the expression of these $sPLA_2$ enzymes (Supplementary Fig. 1c). When we transfected rat mastocytoma RBL-2H3 cells with cDNA encoding PLA2G3 or a catalytically inactive PLA2G3 variant, III-HQ, in which the catalytic-center histidine was replaced with asparagine[23], release of β-hexosaminidase (β-HEX) and generation of PGD_2 induced by crosslinking of FcεRI by IgE and antigen (hereafter called IgE-Ag) was augmented in cells overexpressing native PLA2G3 but not catalytically inactive PLA2G3 (Supplementary Fig. 1d). Thus, PLA2G3 is the main $sPLA_2$ in mouse mast cells, is released by exocytosis and can augment activation of mast cells in a manner dependent upon its enzymatic activity.

Pla2g3 deletion ameliorates mast cell–associated anaphylaxis

Upon passive systemic anaphylaxis (PSA) induced by IgE-Ag, *Pla2g3*$^{+/+}$ and WBB6F1-*Kit*$^{+/+}$ mice, but not mast cell–deficient WBB6F1-*Kit*$^{W/W\text{-}v}$ mice, had much more plasma histamine and a temporary decrease in rectal temperature after systemic antigen challenge, whereas these responses were mild in *Pla2g3*$^{-/-}$ mice (Fig. 2a). Upon PCA induced by IgE-Ag (Fig. 2b and Supplementary Fig. 1e) or compound 48/80 (C48/80; Fig. 2c), edema was markedly lower in *Pla2g3*$^{-/-}$ mice than *Pla2g3*$^{+/+}$ mice. By contrast, transgenic overexpression of human PLA2G3 (*PLA2G3*$^{tg/+}$)[26] augmented both IgE-Ag–dependent (Fig. 2d and Supplementary Fig. 1e) and C48/80-induced (Fig. 2e) PCA as well as IgE-Ag–induced PSA (Fig. 2f). Although the ear skin of *Pla2g3*$^{-/-}$ and *Pla2g3*$^{+/+}$ mice contained an equivalent number of toluidine blue^{+} mast cells, we detected fewer cells showing signs of IgE-Ag–induced degranulation in *Pla2g3*$^{-/-}$ mice than in *Pla2g3*$^{+/+}$ mice (Fig. 2g). Conversely, ears of IgE-Ag–treated *PLA2G3*$^{tg/+}$ mice had more degranulated mast cells than those of replicate control mice despite a similar total mast cell count (Fig. 2h). IgE-Ag–induced PCA in mice lacking other $sPLA_2$ enzymes (*Pla2g2d*$^{-/-}$, *Pla2g2e*$^{-/-}$, *Pla2g2f*$^{-/-}$, *Pla2g5*$^{-/-}$ and *Pla2g10*$^{-/-}$) was similar to that in respective wild-type littermates (Supplementary Fig. 1f).

We immunized *Pla2g3*$^{+/+}$ and *Pla2g3*$^{-/-}$ mice intraperitoneally with alum-adsorbed ovalbumin (OVA) and elicited active cutaneous anaphylaxis by intradermal injection of OVA, which cross-links endogenous IgE-bound FcεRI on mast cells. Under conditions in which serum anti-OVA IgE levels were similar in both genotypes, *Pla2g3*$^{-/-}$ mice exhibited lower local anaphylaxis than did *Pla2g3*$^{+/+}$ mice, as indicated by notable reductions in ear swelling and mast cell degranulation (Fig. 2i–k). Thus, PLA2G3 is the sole $sPLA_2$ isoform associated with mast cell–dependent anaphylaxis.

Pla2g3 deletion impairs maturation of tissue mast cells

Transmission electron microscopy analysis revealed that resting mast cells in *Pla2g3*$^{+/+}$ mice were oval with regular short processes and had many secretory granules filled with electron-lucent and dense contents, whereas those in *Pla2g3*$^{-/-}$ mice had unusual granules that were small and irregular in size, suggesting the immaturity of mast cells (Fig. 3a and Supplementary Fig. 2a). After challenge with antigen, *Pla2g3*$^{+/+}$ skin mast cells exhibited features typical of degranulation, whereas *Pla2g3*$^{-/-}$ mast cells were almost insensitive. In

agreement, the amount of histamine (Fig. 3b) and the expression of *Hdc* (which encodes histidine decarboxylase, a histamine-biosynthetic enzyme; Fig. 3c) were lower in the ears of *Pla2g3*$^{-/-}$ mice than in those of *Pla2g3*$^{+/+}$ mice. Enzymatic activity (Fig. 3d) and expression (Fig. 3e) of mast cell proteases, including chymase (encoded by *Mcpt4*), tryptase (encoded by *Mcpt6*) and carboxypeptidase (encoded by *Cpa3*), were also notably lower in the ears of *Pla2g3*$^{-/-}$ mice relative to *Pla2g3*$^{+/+}$ mice. However, expression of *Kit*, *Mitf* (which encodes a transcription factor essential for mast cell differentiation) and *Srgn* (which encodes serglycin, a proteoglycan core protein) was unchanged in ears of *Pla2g3*$^{-/-}$ mice (Fig. 3e), indicating that not all mast cell markers were affected by PLA2G3 deficiency. We confirmed the lower expression of HDC and the unaltered expression of c-Kit in the skin of *Pla2g3*$^{-/-}$ mice by immunoblotting (Fig. 3f).

Pla2g3$^{-/-}$ pMCs also had smaller and more irregular granules (Fig. 3g and Supplementary Fig. 2b), contained less histamine (Fig. 3h) and exhibited less IgE-Ag–induced histamine release (both amount and percentage; Fig. 3i) than *Pla2g3*$^{+/+}$ pMCs. Although the proportion of Kit^{+}FcεRIα^{+} skin mast cells or pMCs was similar in both genotypes, surface expression of FcεRIα was lower in *Pla2g3*$^{-/-}$ mice than in *Pla2g3*$^{+/+}$ mice (Supplementary Fig. 2c,d). A23187-induced histamine release by *Pla2g3*$^{-/-}$ pMCs was lower in terms of amount, but not percentage, compared to that by *Pla2g3*$^{+/+}$ pMCs (Supplementary Fig. 2e), suggesting that the attenuated IgE-Ag–induced degranulation and anaphylaxis in *Pla2g3*$^{-/-}$ mice was mainly due to the lower histamine content and surface FcεRI expression. Furthermore, intestinal expression of *Mcpt1* and *Mcpt2* (which encode mucosal mast-cell proteases) was markedly lower in *Pla2g3*$^{-/-}$ mice than in *Pla2g3*$^{+/+}$ mice (Supplementary Fig. 2f). Thus, the lower anaphylaxis in *Pla2g3*$^{-/-}$ mice may result from abnormalities in the maturation and degranulation of mast cells in multiple anatomical sites. Other immune-cell populations in the skin and spleen were unaffected by PLA2G3 deficiency (Supplementary Fig. 2g,h).

To assess whether the aberrant features of mast cells in *Pla2g3*$^{-/-}$ mice relied on the absence of PLA2G3 in the mast cells themselves or in mast cell microenvironment, we transferred *Pla2g3*$^{+/+}$ or *Pla2g3*$^{-/-}$ BMMCs intradermally into mast cell–deficient *Kit*$^{W\text{-}sh/W\text{-}sh}$ mice. After 6 weeks, the distribution of mast cells in the ear dermis was comparable between mice reconstituted with *Pla2g3*$^{+/+}$ BMMCs and those reconstituted with *Pla2g3*$^{-/-}$ BMMCs (Supplementary Fig. 3a). Expression of mast-cell marker genes *Hdc*, *Mcpt4*, *Mcpt6* and *Cpa3* (Fig. 3j) and IgE-Ag–mediated PCA (Fig. 3k and Supplementary Fig. 3b) was much greater in the ears of mice that received *Pla2g3*$^{+/+}$ BMMCs over control *Kit*$^{W\text{-}sh/W\text{-}sh}$ mice, whereas these changes were scarcely seen in mice that received *Pla2g3*$^{-/-}$ BMMCs. We observed similar results when we transferred *Pla2g3*$^{+/+}$ or *Pla2g3*$^{-/-}$ BMMCs intravenously into *Kit*$^{W\text{-}sh/W\text{-}sh}$ mice. After 12 weeks of reconstitution, IgE-Ag–mediated PCA was restored in mice reconstituted with *Pla2g3*$^{+/+}$ BMMCs but remained poor in mice reconstituted with *Pla2g3*$^{-/-}$ BMMCs, although we observed similar numbers of reconstituted mast cells in the ear dermis (Supplementary Fig. 3c,d). In these experiments, low levels of mast-cell engraftment in the skin of *Kit*$^{W\text{-}sh/W\text{-}sh}$ mice relative to baseline amounts in the skin of wild-type mice restored PCA efficiently. *Kit*$^{W\text{-}sh/W\text{-}sh}$ mice transferred with *PLA2G3*$^{tg/+}$ BMMCs had a greater PCA response

compared to those transferred with control BMMCs (Supplementary Fig. 3e). Altogether, the defective maturation and activation of mast cells in *Pla2g3*$^{-/-}$ mice are cell autonomous, even though the migration of mast cell progenitors into extravasuclar tissues is not profoundly impaired by PLA2G3 deficiency.

Impaired maturation of *Pla2g3*$^{-/-}$ mast cells in culture

Pla2g3$^{-/-}$ BMMCs grew normally in medium supplemented with IL-3 (Supplementary Fig. 4a) and, unlike tissue-resident mast cells, they had normal surface expression of FcεRIα (Supplementary Fig. 4b). Stimulation with IgE-Ag induced a robust release of sPLA$_2$ activity from wild-type BMMCs, whereas this release was ablated in *Pla2g3*$^{-/-}$ BMMCs and augmented in *PLA2G3*$^{tg/+}$ BMMCs (Supplementary Fig. 4c,d), confirming that PLA2G3 is released upon degranulation. IgE-Ag–stimulated *Pla2g3*$^{-/-}$ BMMCs released less histamine, PGD$_2$ and LTC$_4$ than *Pla2g3*$^{+/+}$ BMMCs, whereas these responses were greater in *PLA2G3*$^{tg/+}$ BMMCs than in control BMMCs (Supplementary Fig. 4e–j). IgE-Ag–induced influx of Ca^{2+}, induction of cytokines (encoded by *Il4*, *Il6* and *Tnf*) and phosphorylation of phospholipase C (PLCγ2) and Akt were similar between the genotypes (Supplementary Fig. 4k–m), suggesting that FcεRI-dependent signaling was not profoundly perturbed by PLA2G3 deficiency. Generation of eicosanoids by mast cells depends on cPLA$_2$α, which is regulated by Ca^{2+}-dependent membrane translocation and MAP kinase-directed phosphorylation[17]. Consistent with the lower generation of eicosanoids (Supplementary Fig. 4f,g), FcεRI-dependent phosphorylation of ERK (not JNK and p38) and cPLA$_2$α and decrease in arachidonic acid–containing phosphatidylcholine were partially impaired in *Pla2g3*$^{-/-}$ BMMCs compared to *Pla2g3*$^{+/+}$ BMMCs, despite the equivalent expression of total ERK and cPLA$_2$α proteins in both cells (Supplementary Fig. 4m–o). Thus, PLA2G3 deficiency attenuates activation of ERK and cPLA$_2$α in BMMCs.

We took advantage of an *in vitro* system in which immature BMMCs undergo maturation toward mature CTMC-like cells in coculture with Swiss 3T3 fibroblasts[27]. PLA2G3 deficiency did not affect the proliferation of BMMCs in coculture (Supplementary Fig. 5a). During coculture, sPLA$_2$ activity was secreted from wild-type BMMCs in response to SCF, whereas sPLA$_2$ secretion was absent in *Pla2g3*$^{-/-}$ BMMCs and augmented in *PLA2G3*$^{tg/+}$ BMMCs (Fig. 4a,b). Although the ultrastructure of *Pla2g3*$^{-/-}$ BMMCs appeared normal, *Pla2g3*$^{-/-}$ CTMC-like cells contained unusual granules with less electron-dense contents than did *Pla2g3*$^{+/+}$ CTMC-like cells (Fig. 4c and Supplementary Fig. 5b). After coculture, the expression of *Hdc* (Fig. 4d) and its product histamine (Fig. 4e) were markedly greater in *Pla2g3*$^{+/+}$ CTMC-like cells, whereas these changes were barely seen in *Pla2g3*$^{-/-}$ cells. Even before coculture, *Hdc* expression and histamine content were slightly lower in *Pla2g3*$^{-/-}$ BMMCs than in *Pla2g3*$^{+/+}$ BMMCs, indicating that some early developmental process had already been perturbed by PLA2G3 deficiency. IgE-Ag–induced histamine release was greater in *Pla2g3*$^{+/+}$ cells after coculture than before coculture, whereas this coculture-driven increase in histamine release was impaired in *Pla2g3*$^{-/-}$ cells (Fig. 4f). Conversely, coculture-induced *Hdc* expression was greater in *PLA2G3*$^{tg/+}$ CTMC-like cells than in control cells (Supplementary Fig. 5c). Supplementation with PLA2G3 in coculture significantly restored the histamine level in *Pla2g3*$^{-/-}$ CTMC-like cells and also elevated it in *Pla2g3*$^{+/+}$ cells (Fig. 4g). *Pla2g3*$^{-/-}$ BMMCs without coculture did not respond to

PLA2G3 (Fig. 4g), suggesting that the action of PLA2G3 on histamine synthesis in mast cells depends on fibroblasts. Histamine content in *Pla2g3*$^{+/+}$ BMMCs without coculture was substantially lower in the presence of PLA2G3 than its absence (Fig. 4g), which might reflect that the enzyme elicits the release of prestored histamine by degranulation (Fig. 1b).

The maturation of wild-type BMMCs to CTMC-like cells increased FcεRI-dependent PGD_2 synthesis (Fig. 4h), with a concomitant increase in *Ptgds2* (hematopoietic PGD_2 synthase; H-PGDS) (Fig. 4i). However, these changes in the PGD_2 pathway occurred only weakly in *Pla2g3*$^{-/-}$ cells. Surface expression of FcεRIα was significantly elevated in *Pla2g3*$^{+/+}$ cells but not in *Pla2g3*$^{-/-}$ cells after coculture (Supplementary Fig. 5d), consistent with the lower surface FcεRIα expression on tissue-resident mast cells in *Pla2g3*$^{-/-}$ mice. The coculture-driven induction of *Mcpt4* and *Mcpt6* (which encode mast cell proteases) and *Ndrg1* (which encodes a mast cell granule–associated protein[27]) was also impaired in *Pla2g3*$^{-/-}$ cells, whereas the constitutive expression of *Srgn* and *Kit* was unaffected (Supplementary Fig. 5e). We verified the attenuated induction of HDC and H-PGDS and the unaltered expression of c-Kit in *Pla2g3*$^{-/-}$ CTMC-like cells at the protein level (Fig. 4j). Although *Pla2g3*$^{+/+}$ CTMC-like cells acquired sensitivity to C48/80 after coculture[27], C48/80-induced degranulation (Fig. 4k) and induction of the putative C48/80 receptors encoded by *Mrgprx1* and *Mrgprx2* (ref. 28; Supplementary Fig. 5e) after coculture were lower in *Pla2g3*$^{-/-}$ cells. The coculture-dependent decrease in *Itga5* (which encodes integrin α_E) and increase in *Icam1* (which encodes integrin β_7), which participates in tissue homing of mast-cell progenitors[6], were unaffected by PLA2G3 deficiency (Supplementary Fig. 5e), consistent with the unaltered number of mast cells in *Pla2g3*$^{-/-}$ tissues. Microarray gene profiling using *Pla2g3*$^{+/+}$ and *Pla2g3*$^{-/-}$ BMMCs before and after coculture revealed that, of the ~41,000 genes examined, *Pla2g3*$^{+/+}$ cells expressed 3,632 coculture-inducible genes, of which 1,409 genes were barely or only partially induced in *Pla2g3*$^{-/-}$ cells. Genes affected by *Pla2g3* ablation included, for example, genes associated with secretory granules, genes related to biosynthesis or receptors for lipid mediators, and genes for cytokines, chemokines and their receptors (Fig. 4l and Supplementary Table 1), underscoring the immaturity of *Pla2g3*$^{-/-}$ cells, particularly after coculture.

By comparison, *Pla2g4a*$^{-/-}$ mice exhibited normal IgE-Ag–induced PCA, with normal counts of dermal mast cells and normal amounts of histamine (Supplementary Fig. 5f–h). IgE-Ag–induced histamine release, cellular histamine content and *Hdc* expression were unaffected by ablation of $cPLA_2\alpha$ (Supplementary Fig. 5i–k). Neither PGD_2 nor LTC_4 was produced by *Pla2g4a*$^{-/-}$ BMMCs (Supplementary Fig. 5l,m), confirming the obligatory role of $cPLA_2\alpha$ in eicosanoid synthesis in mast cells[29]. Thus, the absence of mast cell–derived eicosanoids by $cPLA_2\alpha$ deficiency did not affect maturation, degranulation and anaphylaxis of mast cells, suggesting that the effect of PLA2G3 deficiency on mast cells could not be simply explained by defective synthesis of eicosanoids by mast cells.

PGD_2-DP1 signals mast-cell maturation downstream of PLA2G3

To identify the specific lipid-mediator pathway that lies downstream of PLA2G3, we induced IgE-Ag–dependent PCA on mouse lines deficient in various eicosanoid receptors or biosynthetic enzymes. Of the eicosanoid receptor–deficient mouse lines tested, PCA was

lower only in mice lacking the PGD receptor DP1 (*Ptgdr*$^{-/-}$)[9]. Vascular leakage was lower and ear mast cells exhibited poor degranulation despite an unaltered total count in *Ptgdr*$^{-/-}$ mice compared to wild-type mice (Fig. 5a,b). Dermal mast cells in *Ptgdr*$^{-/-}$ mice had fewer mature secretory granules, contained less histamine and were less sensitive to IgE-Ag–induced degranulation than those in *Ptgdr*$^{+/+}$ mice (Fig. 5c,d). Whereas the PCA was efficiently restored in *Kit*$^{W\text{-}sh/W\text{-}sh}$ mice reconstituted with *Ptgdr*$^{+/+}$ BMMCs, it was restored only partially in those mice reconstituted with *Ptgdr*$^{-/-}$ BMMCs (Fig. 5e). The PCA was unaltered or only slightly augmented in mice lacking other eicosanoid receptors or biosynthetic enzymes (*Ptgdr2*$^{-/-}$, *Ptger1*$^{-/-}$, *Ptger2*$^{-/-}$, *Ptger3*$^{-/-}$, *Ptger4*$^{-/-}$, *Ptgfr*$^{-/-}$, *Ptgir*$^{-/-}$, *Tbxa2r*$^{-/-}$, *Ltb4r1*$^{-/-}$, *Ltb4r2*$^{-/-}$, *Ptges*$^{-/-}$, *Ptges2*$^{-/-}$ and *Alox15*$^{-/-}$; Supplementary Fig. 6a). Although *Ltc4s*$^{-/-}$ mice exhibited a lower PCA response as reported[10], their ear histamine content was unaffected (data not shown). Thus, abnormalities in mast cells observed in mice lacking PLA2G3 were phenocopied only in mice lacking DP1.

Next we examined the expression and function of DP1 in a mast cell–fibroblast coculture system[27]. Although we barely detected *Ptgdr* mRNA in BMMCs and Swiss 3T3 fibroblasts, *Ptgdr* mRNA was robustly induced in *Pla2g3*$^{+/+}$, but not in *Pla2g3*$^{-/-}$, CTMC-like cells after coculture (Fig. 5f). Consistently, *Ptgdr* expression in the ear was lower in *Pla2g3*$^{-/-}$ mice than in *Pla2g3*$^{+/+}$ mice (Fig. 5g). In agreement with the lower histamine amount in *Ptgdr*$^{-/-}$ dermal mast cells (Fig. 5d), the coculture-driven *Hdc* induction was severely impaired in *Ptgdr*$^{-/-}$ CTMC-like cells (Fig. 5h). In addition, the DP1 antagonist BW A868C prevented the coculture-induced upregulation of *Hdc* in wild-type CTMC-like cells (Fig. 5i). Conversely, the DP1 agonist BW 245C significantly enhanced *Hdc* induction in wild-type CTMC-like cells (Fig. 5j). However, the coculture-driven *Hdc* expression was barely restored by BW 245C in *Pla2g3*$^{-/-}$ mice (Fig. 5j), likely because DP1 induction was blunted by PLA2G3 deficiency (Fig. 5f). To circumvent this problem, we used the cAMP-elevating agent forskolin because DP1 is coupled with Gs-cAMP signaling[9]. The addition of forskolin to the coculture bypassed the requirement for DP1 in the induction of *Hdc* in *Pla2g3*$^{-/-}$ CTMC-like cells (Fig. 5k). By comparison, the expression of *Ptgdr2*, which encodes another PGD_2 receptor known as CRTH2, was high in BMMCs and lowered in accordance with their maturation into CTMC-like cells, without being affected by the *Pla2g3* genotypes (Supplementary Fig. 6b). Moreover, *Hdc* induction in CTMC-like cells was unaffected by CRTH2 deficiency in coculture, and *Ptgdr2* expression was unaffected by PLA2G3 deficiency *in vivo* (Supplementary Fig. 6c,d). The coculture-driven production of other eicosanoids such as 15-HETE and PGI_2 was unaffected by PLA2G3 deficiency (Supplementary Fig. 6e). Thus, DP1-cAMP signaling is specifically required for the PLA2G3-dependent maturation of mast cells.

L-PGDS supplies a PGD_2 pool for mast-cell maturation

We hypothesized that the absence of PGD_2 biosynthetic enzyme(s), acting downstream of PLA2G3 and upstream of DP1, would also influence maturation of mast cells. Of the two PGD_2 synthase–encoding genes, *Ptgds2* (which encodes H-PGDS) was expressed in BMMCs but not in Swiss 3T3 fibroblasts, whereas *Ptgds* (which encodes lipocalin-type PGDS; L-PGDS) expression was higher in fibroblasts than in BMMCs (Fig. 6a) and was

below the detection limit in pMCs (data not shown). L-PGDS immunoreactivity was associated with fibroblasts surrounding toluidine blue^{+} mast cells in mouse skin (Supplementary Fig. 7a). PCA was exacerbated in *Ptgds2*$^{-/-}$ mice[30], which lack H-PGDS (Fig. 6b), whereas it was suppressed in *Ptgds*$^{-/-}$ mice[31], which lack L-PGDS (Fig. 6c), in comparison with respective control mice. *Ptgds*$^{-/-}$ mice had fewer degranulated ear mast cells than did *Ptgds*$^{+/+}$ mice after antigen challenge, although the total mast cell count was unaffected (Fig. 6d). Dermal mast cells in *Ptgds*$^{-/-}$ mice were ultrastructurally immature (that is, cytoplasmic granules were small and heterogeneous), comparatively resistant to antigen-induced degranulation, and contained less histamine than those in *Ptgds*$^{+/+}$ mice (Fig. 6e,f). Thus, the notable similarity among *Pla2g3*$^{-/-}$, *Ptgds*$^{-/-}$ and *Ptgdr*$^{-/-}$ mice suggests that PLA2G3, L-PGDS and DP1 may lie in the same regulatory pathway driving maturation of mast cells. The transfer of *Ptgds*$^{+/+}$ or *Ptgds*$^{-/-}$ BMMCs into *Kit*$^{W\text{-}sh/W\text{-}sh}$ mice fully restored the PCA response (Supplementary Fig. 7b), and a similar induction of *Hdc* occurred when *Ptgds*$^{+/+}$ or *Ptgds*$^{-/-}$ BMMCs were cultured with fibroblasts (Supplementary Fig. 7c), indicating that L-PGDS in fibroblasts, not in mast cells, may be important for the regulation of mast cells.

Coculture with L-PGDS–silenced Swiss 3T3 fibroblasts by two distinct *Ptgds*-specific small interfering (si)RNAs resulted in less induction of *Hdc* in wild-type CTMC-like cells (Fig. 6g). PGD_2 generation after coculture of parent fibroblasts with *Pla2g3*$^{-/-}$ BMMCs was ~50% lower than with *Pla2g3*$^{+/+}$ BMMCs (Fig. 6h). The L-PGDS inhibitor AT-56 lowered PGD_2 generation and *Hdc* induction in *Pla2g3*$^{+/+}$ cocultures to amounts similar to those in *Pla2g3*$^{-/-}$ cocultures, although it did not affect these responses in *Pla2g3*$^{-/-}$ cocultures (Fig. 6h,i and Supplementary Fig. 7d). *Hdc* induction in wild-type BMMCs also occurred in coculture with primary skin fibroblasts from *Ptgds*$^{+/+}$ mice, whereas this response was impaired in coculture with those from *Ptgds*$^{-/-}$ mice (Fig. 6j). Thus, the augmentative effects of PLA2G3 on coculture-driven synthesis of PGD_2 and histamine were abrogated when L-PGDS in fibroblasts was ablated. L-PGDS–dependent production of PGD_2, as revealed by coculture of *Ptgds2*$^{-/-}$ BMMCs with Swiss 3T3 fibroblasts, occurred gradually over a long period, whereas H-PGDS–dependent production of PGD_2 was transient, albeit robust (Supplementary Fig. 7e), suggesting that the continuous supply of PGD_2 by L-PGDS is crucial for maturation of mast cells.

Additionally, we observed robust upregulation of *Ptgds2* in BMMCs and *Ptgds* in Swiss 3T3 fibroblasts or in primary mouse skin fibroblasts (and to a much lesser extent in BMMCs) in wild-type BMMC cocultures, whereas these responses occurred only partially in *Pla2g3*$^{-/-}$ BMMC cocultures (Supplementary Fig. 7f–h). Conversely, induction of *Ptgds* in Swiss 3T3 fibroblasts was enhanced in coculture with *PLA2G3*$^{tg/+}$ BMMCs relative to wild-type BMMCs (Supplementary Fig. 7i). Thus, not only did mast cell–derived PLA2G3 supply arachidonic acid to L-PGDS in fibroblasts, it also contributed to induced expression of L-PGDS for efficient biosynthesis of a pool of PGD_2 that promotes maturation of mast cells. However, addition of PLA2G3 or BV-PLA_2 alone did not increase *Ptgds* expression in fibroblasts (Supplementary Fig. 7j), suggesting that some additional mast cell–derived factor(s) may be required for the induction of L-PGDS in fibroblasts. In agreement with the *in vitro* studies, amounts of PGD_2 (Fig. 6k) and expression of two PGDSs (Fig. 6l) were

significantly lower in the ear of *Pla2g3*$^{-/-}$ mice than that of *Pla2g3*$^{+/+}$ mice, confirming the coupling of PLA2G3 with PGD_2 synthesis *in vivo*. Thus, PLA2G3 secreted from mast cells is linked to fibroblastic L-PGDS–dependent synthesis of PGD_2, which in turn activates DP1 induced on mast cells to assist their terminal maturation toward a fully anaphylaxis-sensitive CTMC-like phenotype (Supplementary Fig. 7k).

PLA2G3 PGD_2 axis induces maturation of human mast cells

In human skin, toluidine blue$^+$ dermal mast cells showed PLA2G3 immunoreactivity, although some toluidine blue$^-$ cells also appeared PLA2G3$^+$ (Fig. 7a). We detected *PLA2G3* mRNA expression in mast cells in preference to fibroblasts obtained from human lung and skin (Fig. 7b). *HDC* mRNA expression was robustly induced in human lung mast cells after coculture with human lung fibroblasts, and this induction was suppressed either by anti-PLA2G3, by L-PGDS inhibitor (AT-56) or by DP1 antagonist (BW A868C) to a similar extent (Fig. 7c). Thus, the fibroblast-dependent *HDC* induction in human mast cells also depends on the PLA2G3–L-PGDS–DP1 pathway.

DISCUSSION

Here we showed that PLA2G3, a major $sPLA_2$ in mast cells, contributed to anaphylaxis by inducing maturation of mast cells in concert with adjacent fibroblasts through a unique pathway involving a cell-to-cell loop of the biosynthetic and receptor pathway for PGD_2. Promotion of mast cell maturation by PGD_2-DP1 signaling provides a mechanistic explanation for the protective effect of systemic DP1 ablation on asthma[9]. The paracrine PGD_2 circuit driven by PLA2G3, an ‘anaphylactic $sPLA_2$’, is a previously unidentified lipid-orchestrated pathway linked to allergy and uncovers a missing microenvironmental cue underlying the proper maturation of mast cells.

The SCF–c-Kit system, in cooperation with transcription factors, integrins or accessory cytokines, is essential for the development, homing, proliferation and differentiation of mast cells[3–7]. However, SCF alone is insufficient to drive the full maturation of mast cells, leading to the hypothesis that some other stromal factor(s) may be additionally required. These signals may include, for instance, interleukin 33, nerve growth factor, the morphogen TGF-β, hyaluronic acid and the adhesion molecule SgIGSF (spermatogenic immunoglobulin superfamily)[3,4,7], although their *in vivo* relevancies have not yet been fully understood. As in mice lacking PLA2G3, mast cells in mice lacking histamine (*Hdc*$^{-/-}$) or heparin (*Ndst2*$^{-/-}$ or *Srgn*$^{-/-}$) are immature and have low histamine content[32–34], suggesting that the lower amount of histamine may underlie, at least in part, the defective maturation of mast cells. We showed here that a signal driven by PGD_2, a bioactive lipid, is a missing link required for the fibroblast-driven maturation of mast cells. The PLA2G3–L-PGDS–DP1 circuit revealed the paracrine action of $sPLA_2$ in the biosynthetic mobilization of PGD_2 by proximal cells, the functional segregation of the two PGDS enzymes in distinct cell populations and a new aspect of PGD_2-DP1 signaling in promoting maturation of mast cells and thereby allergy. Moreover, our results revealed a previously unidentified aspect of the stromal cytokine SCF, which triggers this unique lipid-driven pathway by inducing PLA2G3 secretion from mast cells.

L-PGDS, a fibroblast-cell enzyme, acts downstream of PLA2G3 to supply PGD_2 to DP1 in mast cells to drive their terminal maturation. Contrary to our prediction, PGD_2 driven by H-PGDS, a mast cell enzyme, had an anti-allergy role, a view that is consistent with the exacerbated allergen-induced contact dermatitis in *Ptgds2*$^{-/-}$ mice[11]. Although it is unclear how the L-PGDS–driven extrinsic, but not the H-PGDS–driven intrinsic, pool of PGD_2 is preferentially used by DP1 on mast cells, we speculate that the prolonged supply of PGD_2 by L-PGDS, rather than its transient supply by H-PGDS, may be suitable for a long-lasting cell differentiation process. Alternatively, the PGD_2 captured by L-PGDS, a lipid carrier protein (lipocalin), may be stabilized or better presented to mast cell DP1. This idea is reminiscent of a finding that lysophosphatidic acid (LPA), another lipid mediator, is presented to its cognate receptor as a complex with autotaxin, an LPA-producing enzyme[35]. The spatiotemporal discrimination of distinct PGD_2 pools is also supported by the fact that although PGD_2 promotes Th2-based asthma[9], it contributes to resolution of inflammation through limiting neutrophil infiltration, dendritic cell activation or other mechanisms[11–13].

The paracrine PLA2G3–L-PGDS–DP1 circuit could not be compensated by other PLA_2 enzymes, implying a specific role of this atypical $sPLA_2$. We observed no defects in maturation of mast cells or anaphylaxis even in mice lacking $cPLA_2\alpha$, although mild developmental changes in *Pla2g4a*$^{-/-}$ BMMCs have been reported, probably because of different culture conditions[29]. Presumably, ablation of only the specific and local lipid mediator pathway by PLA2G3 deficiency, in contrast to ablation of bulk eicosanoids in both mast cells and microenvironments by $cPLA_2\alpha$ deficiency[29], may have a different impact on mast cells. The phenotypes observed in *Pla2g3*$^{-/-}$ mice tend to be more severe than those observed in *Ptgdr*$^{-/-}$ or *Ptgds*$^{-/-}$ mice, suggesting that PLA2G3 might be also coupled with other lipid signal(s) that could act in concert with the L-PGDS–DP1 axis to promote full maturation of mast cells. Such lipid candidates include LPA and lysophosphatidylserine, which can affect mast cell development and activation[36,37]. Not only can lysophospholipids transmit signals through their specific receptors, but they can also facilitate the opening of Ca^{2+} channels, which might explain the degranulation-promoting effect of PLA2G3 on mast cells.

Although it has been proposed that $sPLA_2$ enzymes, after being secreted, may act on neighboring cells or extracellular phospholipids to augment lipid mediator biosynthesis, this idea has yet to gain traction because *in vivo* evidence is largely lacking. Our study provides to our knowledge the first clear *in vivo* evidence that $sPLA_2$ acts in this manner, thus providing a rationale for the long-standing question on the role of the secreted type of PLA_2. This extracellular PLA_2 family, through a paracrine process, regulates homeostasis and pathology in response to a given microenvironmental cue. Given that PLA2G3 is insensitive to classical $sPLA_2$ inhibitors, a new agent that specifically inhibits this unique $sPLA_2$ may be useful for the treatment of patients with mast cell–associated allergic and other diseases.

ONLINE METHODS

Mice

Pla2g3$^{-/-}$, *Pla2g4a*$^{-/-}$, *Pla2g5*$^{-/-}$, *Pla2g10*$^{-/-}$, *Ptgdr*$^{-/-}$, *Ptgdr2*$^{-/-}$, *Ptgds*$^{-/-}$, *Ptgds2*$^{-/-}$, *Ptges*$^{-/-}$, *Ptger1*$^{-/-}$, *Ptger2*$^{-/-}$, *Ptger3*$^{-/-}$, *Ptger4*$^{-/-}$, *Ptgfr*$^{-/-}$, *Ptgir*$^{-/-}$, *Tbxa2r*$^{-/-}$,

Ltb4r1$^{-/-}$, *Ltb4r2*$^{-/-}$, *Ltc4s*$^{-/-}$, *Alox15*$^{-/-}$ *and PLA2G3*$^{tg/+}$ mice have been described previously[9,14,17–19,22,26,38–44]. *Ptges2*$^{-/-}$ mice (RIKEN RBRC04849) were generated by the Institute of Resource Development and Analysis (Kumamoto University). *Pla2g2d*$^{-/-}$, *Pla2g2e*$^{-/-}$ and *Pla2g2f*$^{-/-}$ mice were generated by the Transgenic Resources Program (Department of Comparative Medicine, University of Washington; unpublished data). These mice were backcrossed to C57BL/6 mice for more than 11 generations, except for *Pla2g3*$^{-/-}$ and *Ptger4*$^{-/-}$ mice (129Sv × C57BL/6), which were from the third backcrosses to C57BL/6 mice owing to severe problems in reproduction[22] and neonatal death[39], respectively, particularly after successive backcrossing onto the C57BL/6 background. All experiments using knockout or transgenic mice (male, 8–12-week-old) were compared with their age-matched littermate control mice. Mast cell–deficient *Kit* mutant mice, C57BL/6J-*Kit*$^{W\text{-}sh/W\text{-}sh}$ and WBB6F$_1$-*Kit*$^{W/W\text{-}v}$, were purchased from the Jackson Laboratories and Japan SLC, respectively. All mice were housed in climate-controlled (23 °C) specific pathogen–free facilities with a 12-h light-dark cycle, with free access to standard laboratory food (CE2; CLEA) and water. All animal experiments were performed in accordance with protocols approved by the Institutional Animal Care and Use Committees of the Tokyo Metropolitan Institute of Medical Science and Showa University, in accordance with the Standards Relating to the Care and Management of Experimental Animals in Japan.

PLA$_2$ assay

BV-PLA$_2$ was purchased from Sigma-Aldrich. Recombinant mature human PLA2G3 protein was expressed in silkworms by the baculo-virus system and purified to near homogenity by an affinity column conjugated with mouse monoclonal anti–human PLA2G3 (5D2F1; IgG), as described previously[26]. PLA$_2$ activities in the supernatants of mast cells were assayed by measuring the amounts of [^{14}C]linoleic acid released from 1-palmitoyl-2-[^{14}C]linoleoyl-phosphatidylethanolamine (Perkin Elmer). Each reaction mixture consisted of appropriate amounts of the samples, 100 mM Tris-HCl (pH 7.4), 4 mM $CaCl_2$ and the substrate at 1 μM. After incubation for 2 h at 37 °C, [^{14}C]linoleic acid was extracted, and the radioactivity was quantified with a liquid scintillation counter (LS5801; Beckman), as described previously[22–24].

Anaphylaxis

For PSA, mice were intravenously injected with 3 μg of monoclonal anti-DNP IgE (SPE-7; Sigma-Aldrich). After 24 h, the mice were challenged intravenously with 25 or 500 μg of DNP-conjugated human serum albumin (HSA; Sigma-Aldrich)[27]. Then, the rectal temperature was measured for 120 min with an electronic thermometer (Physitemp Instruments). For PCA, mice were passively sensitized by intradermal injection with 30 ng of anti-DNP IgE. After 24 h, the mice were challenged by intravenous injection of 20 or 60 μg of DNP-HSA in saline containing Evans blue dye (Wako)[27]. Extravasation of blue dye in the ear was monitored for 30 min, and ear biopsies were incubated at 37 °C in 3 N KOH. Quantitative analysis of the extracts was performed by measuring the absorbance of blue dye at 620 nm. For active anaphylaxis, mice were immunized intraperitoneally on days 0 (day when OVA was first administered), 7 and 14 with 10 μg of chicken OVA (Sigma-Aldrich) in 100 μl of saline mixed with 200 μl of alum (Alu Gel S, which contained 2% $Al(OH)_3$; Serva). Seven days after the last immunization, the left and right ears of mice were injected

intradermally with 30 μg of OVA. Net ear swelling was measured at 30 min after challenge with OVA.

Measurement of histamine and protease activities

The procedures were described previously[27]. Briefly, tissues were homogenized in PBS with a bead crusher (μT-01; Taitec) at 4 °C, and Triton X-100 was added to a final concentration of 0.5% (v/v). For the histamine assay, the lysates were treated with 3% (v/v) perchloric acid and left for 30 min on ice, and the resulting supernatants (tissue extracts) after centifugation at 10,000*g* for 30 min at 4 °C were applied to a cation-exchange WCX-1 column on HPLC (Shimadzu) to separate histamine, which was then measured fluorometrically by the *o*-phthalaldehyde method[45]. For the protease assay, 10 μl of the tissue extracts were diluted with 90 μl of 50 mM Tris-HCl (pH 8.3), followed by incubation with 20 μl of 1.8 mM chromogenic substrates for chymotrypsin- or trypsin-like proteases (S-2586 and S-2288, respectively; Chromogenix) and CPA (M-2245; Bachem) at 37 °C for 1–3 min. Changes in absorbance at 405 nm were measured.

Culture of mouse BMMCs and other bone marrow–derived cells

To prepare BMMCs, mouse bone marrow (BM) cells were cultured in IL-3–containing BMMC complete medium[27]. After 4–6 weeks of culture, >97% of the cells were identified as $Kit^+Fc\varepsilon RI\alpha^+$ mast cells by flow cytometry. The coculture-driven maturation of immature BMMCs toward CTMC-like cells has been described previously[27]. Briefly, BMMCs were seeded onto Swiss 3T3 fibroblast monolayer and cocultured for the appropriate durations (typically for 4 d) in the presence of mouse SCF (100 ng/ml; Peprotech). The cells were trypsinized and reseeded in culture dishes, and nonadherent cells were collected. Purity (>99%) was confirmed by flow cytometry for Kit and FcεRIα. Maturation of BMMCs into CTMC-like cells was verified by staining their granules with alcian blue and counterstaining with safranin O. As required for experiments, 10 μM AT-56, 1 μM BW A868C, 10 μM BW 245C (Cayman Chemical) or 10 μM forskolin (Sigma-Aldrich) were added to the coculture.

BM cells were cultured with mouse granulocyte-macrophage colony stimulating factor (GM-CSF; 10 ng/ml; Peprotech) for 9 d, mouse macrophage colony stimulating factor (M-CSF; 100 ng/ml; Kyowa Kirin) for 3 d or mouse TSLP (1 μg/ml; R&D Systems) for 5 d in RPMI1640 medium (Invitrogen) containing 10% (v/v) FBS (Invitrogen) to obtain BMDCs, BMDMs or BM basophils, respectively[46,47]. The purity of each cell population was verified by flow cytometry for the expression of CD11c and MHC class II for BMDCs, the expression of F4/80 and CD11b for BMDMs, and the expression of FcεRIα and CD200R3 (or DX5α) coupled with a lack of expression of Kit for BM basophils (see below).

Activation of BMMCs

BMMCs (10^6 cells) before and after coculture with fibroblasts were sensitized with 1 μg/ml anti-DNP IgE for 2 h and then stimulated with various concentrations (typically 100 ng/ml) of DNP-BSA (Sigma-Aldrich), 100 ng/ml mouse SCF or 10 μg/ml C48/80 (Sigma-Aldrich). Degranulation was evaluated by measuring histamine or β-HEX release, as described previously[27]. The levels of eicosanoids were determined by ELISA in accordance with the manufacturer's instructions (Cayman Chemical). Expression of cytokines was assessed by

real-time PCR. Lactate dehydrogenase activity was measured using an LDH Cytotoxicity Detection Kit (Takara).

Preparation and activation of mouse pMCs

To collect peritoneal cells, 5 ml of Hank's balanced salt solution (Invitrogen) was injected into the mouse peritoneal cavity, and the abdomen was massaged gently. After collecting peritoneal cells from the peritoneal fluid, they were resuspended in PIPES-buffered saline for electron microscopy or in BMMC-complete medium for degranulation assay. For degranulation, 10^6 cells were treated for 30 min with 1–5 μg/ml of human PLA2G3 or BV-PLA_2, with 1 μM A23187 (Sigma-Aldrich), or with 1 μg/ml anti-DNP IgE for 1 h and then with 100 ng/ml DNP-BSA for 30 min in the presence of 4 μM lysophosphatidylserine (Avanti Polar Lipids). The release of histamine was then evaluated.

Preparation of mouse skin mast cells and fibroblasts

Mouse ear skin was dispersed with 1.6 mg/ml collagenase type II (Worthington) and 0.1 mg/ml DNase I (Sigma-Aldrich) in RPMI1640 containing 10% FBS for 30 min at 37 °C and passed through a cell strainer (40-μm mesh size). Skin mast cells were identified as $Kit^+Fc\varepsilon RI\alpha^+$ cells after CD45 gating by flow cytometry. The skin-dispersed cells were cultured in RPMI1640 containing 10% FBS, trypsinized and reseeded on culture dishes, and adherent cells grown to confluency were used as skin fibroblasts.

Preparation and culture of human mast cells and fibroblasts

Preparation and culture of mast cells from human skin and lung were performed as described previously[48]. Briefly, macroscopically normal human lung or skin tissue was obtained during surgery at the Nihon University Hospital under approval of the faculty ethics committee and informed consent from the patient. Lung and skin cells were dispersed from chopped lung and foreskin specimens by collagenase and hyaluronidase (Sigma-Aldrich). These cells were maintained for 6 weeks in MethoCult SF^{BIT} (Iscove's modified Dulbecco's medium (IMDM)-based serum-free medium containing 1.2% (w/v) methylcellulose; Veritas) supplemented with human SCF (100 ng/ml; Peprotech) and human IL-6 (50 ng/ml; Peprotech). On day 42, methylcellulose was dissolved in PBS, and the cells were resuspended and cultured in IMDM medium (Invitrogen) containing 0.1% BSA, 100 ng/ml SCF and 50 ng/ml IL-6. The purity of human mast cells, as assessed with metachromatic staining, was more than 97%. Human skin and lung fibroblasts (CC-2511 and CC-2512, respectively) and their culture medium were purchased from Lonza. Human lung mast cells (5×10^5 cells) were seeded onto the human lung fibroblast monolayer and cocultured for 4 d in 500 μl of IMDM medium plus 2% FBS in the presence of SCF and IL-6, with medium change at 2-d intervals. The cells were trypsinized and reseeded in culture dishes, and nonadherent cells were collected. The purity of mast cells was normalized based on the expression of *KIT*.

Real-time PCR

Total RNA was extracted from tissues and cells using TRIzol reagent (Invitrogen). First-strand cDNA synthesis was performed using the High-Capacity cDNA Reverse-

Transcriptase Kit (Applied Biosystems). PCRs were carried out using the TaqMan Gene Expression System (Applied Biosystems) on an ABI7700 Real-Time PCR system (Applied Biosystems). The probe-primer sets are listed in Supplementary Table 2.

Measurement of intracellular Ca^{2+} levels

Intracellular Ca^{2+} levels were measured as described previously[27]. Briefly, IgE-sensitized BMMCs on coverslips were loaded for 60 min with the fluorescent Ca^{2+} indicator fura-2/AM (5 μM; Invitrogen) in Tyrode-HEPES buffer (pH 7.4) containing 2.5 mM probenecid, 0.04% (v/v) pluronic acid and 1% (v/v) serum. Then, the cells were washed and stimulated with antigen. Fura-2 fluorescence images were obtained using an image analyzer (ARGUS-50; Hamamatsu Photonics) with excitation at 340 nm (F340) and 380 nm (F380) at 5-s intervals. The fluorescence ratio (F340/F380) was calculated using US National Institutes of Health ImageJ software.

Western blotting

Tissue homogenates (20 μg protein equivalent) or BMMCs (2×10^5 cells) were lysed in SDS-PAGE sample buffer (63 mM Tris-HCl (pH 6.8), 2% (w/v) SDS, 10% (v/v) glycerol, and 0.08% (w/v) bromophenol blue) containing 5% (v/v) 2-mercaptoethanol, and then subjected to SDS-PAGE. Proteins were subsequently blotted onto PVDF membranes (Bio-Rad), followed by blocking with 5% (w/v) milk powder in PBS containing 0.05% (v/v) Tween 20 (PBS-T). The membranes were probed with rabbit polyclonal antibodies to HDC[49], H-PGDS[30], Kit (18101; IBL), PLCγ2 (3872; Cell Signaling), phospho-PLCγ2 Y1217 (3871; Cell Signaling), $cPLA_2\alpha$ (2832; Cell Signaling) or phospho-$cPLA_2\alpha$ S505 (2831; Cell Signaling) or mouse monoclonal antibodies against Akt (D9E; Cell Signaling), phospho-Akt S473 (C67E7; Cell Signaling), ERK1/2 (MK12; BD Transduction Laboratories), phospho-ERK1/2 T202/Y204 (20A; BD Transduction Laboratories), JNK (37; BD Transduction Laboratories), phospho-JNK T183/Y185 (41; BD Transduction Laboratories), p38 (27; BD Transduction Laboratories) or phospho-p38 MAPK T180/Y182 (30; BD Transduction Laboratories) at 1:500–1:2,000 dilutions in PBS-T containing 1% (w/v) milk powder or in Can Get Signal Solution 1 (Toyobo) for 1.5 h. After membranes were washed, the membranes were incubated for 1 h with horseradish peroxidase (HRP)-conjugated anti-rabbit (AP156P; Chemicon) or anti-mouse (21040; Molecular Probes) IgG at 1:5,000 dilution in PBS-T containing 1% milk powder or in Can Get Signal Solution 2 (Toyobo), and then visualized with ECL Prime western blotting detection reagent (GE Healthcare Life Science) on LAS-4000 (Fuji Film).

Histological analysis

Ears were fixed in 10% (v/v) neutral buffered formalin, embedded in paraffin and cut using a microtome. The sections (4 μm thickness) were stained with 0.05% toluidine blue (pH 0.5) for the detection of mast cells. Degranulated mast cells were defined as those showing the release of cellular granules. For immunohistochemistry, sections were incubated in PBS containing 5% normal goat serum, 5% BSA and 0.025% Triton X-100 for 20 min and then immunostained with a rabbit polyclonal to human PLA2G3, which reacts with both mature human and mouse enzymes (whose homology is 83%)[22–24], and mouse L-PGDS[50], at dilutions of 1:200 and 1:1,000, respectively, in the same buffer at 4 °C overnight. These

preparations were incubated with biotinylated goat anti-rabbit IgG (BA-1000; Vector Laboratories) in PBS containing 5% BSA, 0.025% Triton X-100 and 10% mouse serum for 30 min followed by incubation with avidin DH and biotinylated HRP (Vectastain ABC kit; Vector Laboratories). These preparations were stained with 0.5 mg/ml 3,3′-diaminobenzidine and 0.1% (v/v) hydrogen peroxide solution. Human tissue sections were obtained from Chiba University following approval by the faculty ethical committee and informed consent from the patient. For transmission microscopy, tissues or cells were fixed with 0.1 M sodium cacodylate buffer (pH 7.2) containing 1% (v/v) glutaraldehyde and 4% (w/v) paraformaldehyde, postfixed with 2% (w/v) OsO_4 in PBS, dehydrated by a graded ethanol series, passed through propylene oxide and embedded in Poly/Bed812 EPON (Polyscience). Ultrathin sections (0.08-μm thickness) were stained with uranyl acetate and lead citrate and then examined using an electron microscope (H-7600; Hitachi).

Adoptive transfer of BMMCs into mast cell–deficient mice

BMMCs obtained from 8–12-week-old male mice were reconstituted by intradermal (10^6 cells) or intravenous (10^7 cells) injection into 6-week-old male *Kit*$^{W\text{-}sh/W\text{-}sh}$ mice. Six weeks after intradermal transfer or 12 weeks after intravenous transfer of BMMCs, the mice were subjected to IgE-Ag–induced PCA, as described above. Alternatively, mast cells from the base to the tip of the ears from these mice were evaluated by toluidine blue staining or by real-time PCR of mast cell marker genes.

Flow cytometry

Cells were stained with either a labeled monoclonal antibody or an isotype-matched control antibody (hamster IgG (HTK888), mouse IgG_1 (MOPC-21), rat IgG_{2a} (RTK2758) or rat IgG_{2b} (RTK4530); BioLegend) and analyzed by flow cytometry using FACSCalibur (BD Biosciences) or FACSAria III Cell Sorter (BD Biosciences) with FlowJo software (Tree Star). The antibodies used were specific for mouse Kit (2B8; BD Biosciences), FcεRIα (MAR-1; eBioscience), DX5 (DX5; eBioscience), CD200R3 (Ba13; BioLegend), CD45 (30-F11; eBioscience), CD11c (N418; eBioscience), MHC class II (M5/114.15.2; eBioscience), CD11b (M1/70; BioLegend), F4/80 (BM8; BioLegend), CD45R/B220 (RA3-6B2; BD Biosciences), CD3ε (145-2X11; eBioscience), Gr-1 (RB-8C5; BioLegend), FOXP3 (150D; BioLegend) and FR4 (12A5; BioLegend).

Microarray

Total RNA was extracted from BMMCs derived from *Pla2g3*$^{-/-}$ and *Pla2g3*$^{+/+}$ mice before and after coculture and purified using the RNeasy Mini Kit (Qiagen). The quality of RNA was assessed with a 2100 Bioanalyzer (Agilent Technologies). Both cDNA and cRNA were synthesized with a Low Input Quick Amp Labeling Kit according to the manufacturer's protocol (Agilent Technologies). Samples were hybridized to the Whole Mouse Genome Microarray Kit (4 × 44K; Agilent Technologies), washed and then scanned using a Laser Scanner GenePix 4000B (Molecular Devices). Microarray data were analyzed with Feature Extraction software (Agilent Technologies) and then imported into GeneSpringGX11.5 (Agilent Technologies). Probes were normalized by quantile normalization among all microarray data.

RNA interference

Swiss 3T3 fibroblasts were cultured in 12-well plates to 50% confluence and transfected with a Mission predesigned siRNA construct (20 nM) for *Ptgds* (SASI_Mm01_00116073 or 00116081; Sigma-Aldrich) or a scrambled control siRNA (Invitrogen) using oligofectamine (Invitrogen), according to the manufacturer's instructions. After 48 h, wild-type BMMCs were cocultured for 2 d with the transfected cells.

Electrospray ionization mass spectrometry (ESI-MS)

ESI-MS lipidomics analysis using a 4000Q TRAP quadrupole-linear ion trap hybrid mass spectrometer (AB SCIEX) with an UltiMate 3000 nano/cap/micro-liquid chromatography system (Dionex Corporation) combined with an HTS PAL autosampler (CTC Analytics AG) was performed as described previously[44]. Briefly, phospholipids extracted from 10^7 BMMCs were subjected directly to ESI-MS analysis by flow injection; typically, 3 μl (3 nmol phosphorous equivalent) of sample was applied. The mobile phase composition was acetonitrile/methanol/water (v/v/v = 6/7/2) plus 0.1% (v/v) ammonium formate (pH 6.8) at a flow rate of 10 μl/min. The scan range of the instrument was set at *m*/*z* 200–1,000 at a scan speed of 1,000 Da/s. The trap fill-time was set at 3 ms in the positive ion mode and at 5 ms in the negative ion mode. The ion spray voltage was set at 5,500 V in the positive ion mode and at −4,500 V in the negative ion mode. Nitrogen was used as a curtain gas (at a setting of 10 arbitrary units) and as a collision gas (set to 'high').

Statistical analysis

The Excel Statistical Program File ystat 2008 (Igaku Tosho Shuppan) was used to determine statistical significance evaluated by an unpaired Student's *t*-test for two groups or an analysis of variance (ANOVA) for multiple groups. *P* values of less than 0.05 and 0.01 were considered statistically significant. Data are presented as the mean ± s.e.m.

Supplementary Material

Refer to Web version on PubMed Central for supplementary material.

Acknowledgments

We thank Y. Tanoue, H. Ohkubo, K. Araki and K. Yamamura for generating *Ptges2*$^{-/-}$ mice. This work was supported by grants-in-aid for Scientific Research from the Ministry of Education, Culture, Sports, Science and Technology of Japan (22116005 and 24390021 to M.M. and 23790119 and 24117724 to Y.T.), Promoting Individual Research to Nurture the Seeds of Future Innovation and Organizing Unique Innovative Network (PRESTO) of Japan Science and Technology Agency (to M.M.), and the Uehara, Mitsubishi, Terumo, Mochida and Toray Science Foundations (to M.M.).

References

1. Galli SJ, Tsai M. IgE and mast cells in allergic disease. Nat Med. 2012; 18:693–704. [PubMed: 22561833]
2. Gurish MF, Austen KF. Developmental origin and functional specialization of mast cell subsets. Immunity. 2012; 37:25–33. [PubMed: 22840841]
3. Allakhverdi Z, Smith DE, Comeau MR, Delespesse G. Cutting edge: The ST2 ligand IL-33 potently activates and drives maturation of human mast cells. J Immunol. 2007; 179:2051–2054. [PubMed: 17675461]

4. Matsuda H, et al. Nerve growth factor induces development of connective tissue-type mast cells *in vitro* from murine bone marrow cells. J Exp Med. 1991; 174:7–14. [PubMed: 1711569]
5. Abonia JP, et al. Constitutive homing of mast cell progenitors to the intestine depends on autologous expression of the chemokine receptor CXCR2. Blood. 2005; 105:4308–4313. [PubMed: 15705791]
6. Gurish MF, et al. Intestinal mast cell progenitors require CD49dβ7 (α4β7 integrin) for tissue-specific homing. J Exp Med. 2001; 194:1243–1252. [PubMed: 11696590]
7. Ito A, et al. SgIGSF: a new mast-cell adhesion molecule used for attachment to fibroblasts and transcriptionally regulated by MITF. Blood. 2003; 101:2601–2608. [PubMed: 12456501]
8. Shimizu T. Lipid mediators in health and disease: enzymes and receptors as therapeutic targets for the regulation of immunity and inflammation. Annu Rev Pharmacol Toxicol. 2009; 49:123–150. [PubMed: 18834304]
9. Matsuoka T, et al. Prostaglandin D_2 as a mediator of allergic asthma. Science. 2000; 287:2013–2017. [PubMed: 10720327]
10. Kanaoka Y, Maekawa A, Penrose JF, Austen KF, Lam BK. Attenuated zymosan-induced peritoneal vascular permeability and IgE-dependent passive cutaneous anaphylaxis in mice lacking leukotriene C_4 synthase. J Biol Chem. 2001; 276:22608–22613. [PubMed: 11319240]
11. Trivedi SG, et al. Essential role for hematopoietic prostaglandin D_2 synthase in the control of delayed type hypersensitivity. Proc Natl Acad Sci USA. 2006; 103:5179–5184. [PubMed: 16547141]
12. Hammad H, et al. Activation of the D prostanoid 1 receptor suppresses asthma by modulation of lung dendritic cell function and induction of regulatory T cells. J Exp Med. 2007; 204:357–367. [PubMed: 17283205]
13. Levy BD, Clish CB, Schmidt B, Gronert K, Serhan CN. Lipid mediator class switching during acute inflammation: signals in resolution. Nat Immunol. 2001; 2:612–619. [PubMed: 11429545]
14. Kunikata T, et al. Suppression of allergic inflammation by the prostaglandin E receptor subtype EP3. Nat Immunol. 2005; 6:524–531. [PubMed: 15806106]
15. Serhan CN, Chiang N, Van Dyke TE. Resolving inflammation: dual anti-inflammatory and pro-resolution lipid mediators. Nat Rev Immunol. 2008; 8:349–361. [PubMed: 18437155]
16. Murakami M, et al. Recent progress in phospholipase A_2 research: From cells to animals to humans. Prog Lipid Res. 2011; 50:152–192. [PubMed: 21185866]
17. Uozumi N, et al. Role of cytosolic phospholipase A_2 in allergic response and parturition. Nature. 1997; 390:618–622. [PubMed: 9403692]
18. Munoz NM, et al. Deletion of secretory group V phospholipase A_2 attenuates cell migration and airway hyperresponsiveness in immunosensitized mice. J Immunol. 2007; 179:4800–4807. [PubMed: 17878379]
19. Henderson WR Jr, et al. Importance of group X-secreted phospholipase A_2 in allergen-induced airway inflammation and remodeling in a mouse asthma model. J Exp Med. 2007; 204:865–877. [PubMed: 17403936]
20. Bilo BM, Rueff F, Mosbech H, Bonifazi F, Oude-Elberink JN. Diagnosis of Hymenoptera venom allergy. Allergy. 2005; 60:1339–1349. [PubMed: 16197464]
21. Dudler T, et al. A link between catalytic activity, IgE-independent mast cell activation, and allergenicity of bee venom phospholipase A_2. J Immunol. 1995; 155:2605–2613. [PubMed: 7544378]
22. Sato H, et al. Group III secreted phospholipase A_2 regulates epididymal sperm maturation and fertility in mice. J Clin Invest. 2010; 120:1400–1414. [PubMed: 20424323]
23. Murakami M, et al. Cellular distribution, post-translational modification, and tumorigenic potential of human group III secreted phospholipase A_2. J Biol Chem. 2005; 280:24987–24998. [PubMed: 15863501]
24. Murakami M, et al. Cellular arachidonate-releasing function of novel classes of secretory phospholipase A_2s (groups III and XII). J Biol Chem. 2003; 278:10657–10667. [PubMed: 12522102]
25. Valentin E, Ghomashchi F, Gelb MH, Lazdunski M, Lambeau G. Novel human secreted phospholipase A_2 with homology to the group III bee venom enzyme. J Biol Chem. 2000; 275:7492–7496. [PubMed: 10713052]

26. Sato H, et al. Analyses of group III secreted phospholipase A_2 transgenic mice reveal potential participation of this enzyme in plasma lipoprotein modification, macrophage foam cell formation, and atherosclerosis. J Biol Chem. 2008; 283:33483–33497. [PubMed: 18801741]
27. Taketomi Y, et al. Impaired mast cell maturation and degranulation and attenuated allergic responses in *Ndrg1*-deficient mice. J Immunol. 2007; 178:7042–7053. [PubMed: 17513753]
28. Kashem SW, et al. G protein coupled receptor specificity for C3a and compound 48/80-induced degranulation in human mast cells: roles of Mas-related genes MrgX1 and MrgX2. Eur J Pharmacol. 2011; 668:299–304. [PubMed: 21741965]
29. Nakatani N, et al. Role of cytosolic phospholipase A_2 in the production of lipid mediators and histamine release in mouse bone-marrow-derived mast cells. Biochem J. 2000; 352:311–317. [PubMed: 11085923]
30. Mohri I, et al. Prostaglandin D_2-mediated microglia/astrocyte interaction enhances astrogliosis and demyelination in twitcher. J Neurosci. 2006; 26:4383–4393. [PubMed: 16624958]
31. Eguchi N, et al. Lack of tactile pain (allodynia) in lipocalin-type prostaglandin D synthase-deficient mice. Proc Natl Acad Sci USA. 1999; 96:726–730. [PubMed: 9892701]
32. Ohtsu H, et al. Mice lacking histidine decarboxylase exhibit abnormal mast cells. FEBS Lett. 2001; 502:53–56. [PubMed: 11478947]
33. Forsberg E, et al. Abnormal mast cells in mice deficient in a heparin-synthesizing enzyme. Nature. 1999; 400:773–776. [PubMed: 10466727]
34. Humphries DE, et al. Heparin is essential for the storage of specific granule proteases in mast cells. Nature. 1999; 400:769–772. [PubMed: 10466726]
35. Nishimasu H, et al. Crystal structure of autotaxin and insight into GPCR activation by lipid mediators. Nat Struct Mol Biol. 2011; 18:205–212. [PubMed: 21240269]
36. Bagga S, et al. Lysophosphatidic acid accelerates the development of human mast cells. Blood. 2004; 104:4080–4087. [PubMed: 15319282]
37. Iwashita M, et al. Synthesis and evaluation of lysophosphatidylserine analogues as inducers of mast cell degranulation. Potent activities of lysophosphatidylthreonine and its 2-deoxy derivative. J Med Chem. 2009; 52:5837–5863. [PubMed: 19743861]
38. Satoh T, et al. Prostaglandin D_2 plays an essential role in chronic allergic inflammation of the skin via CRTH2 receptor. J Immunol. 2006; 177:2621–2629. [PubMed: 16888024]
39. Segi E, et al. Patent ductus arteriosus and neonatal death in prostaglandin receptor EP4-deficient mice. Biochem Biophys Res Commun. 1998; 246:7–12. [PubMed: 9600059]
40. Sugimoto Y, et al. Failure of parturition in mice lacking the prostaglandin F receptor. Science. 1997; 277:681–683. [PubMed: 9235889]
41. Kobayashi T, et al. Roles of thromboxane A_2 and prostacyclin in the development of atherosclerosis in *apoE*-deficient mice. J Clin Invest. 2004; 114:784–794. [PubMed: 15372102]
42. Iizuka Y, et al. Protective role of the leukotriene B_4 receptor BLT2 in murine inflammatory colitis. FASEB J. 2010; 24:4678–4690. [PubMed: 20667973]
43. Sun D, Funk CD. Disruption of 12/15-lipoxygenase expression in peritoneal macrophages. Enhanced utilization of the 5-lipoxygenase pathway and diminished oxidation of low density lipoprotein. J Biol Chem. 1996; 271:24055–24062. [PubMed: 8798642]
44. Ueno N, et al. Analysis of two major intracellular phospholipases A_2 (PLA_2) in mast cells reveals crucial contribution of cytosolic $PLA_2\alpha$, not Ca^{2+}-independent $PLA_2\beta$, to lipid mobilization in proximal mast cells and distal fibroblasts. J Biol Chem. 2011; 286:37249–37263. [PubMed: 21880721]
45. Shore PA, Burkhalter A, Cohn VH Jr. A method for the fluorometric assay of histamine in tissues. J Pharmacol Exp Ther. 1959; 127:182–186. [PubMed: 14446178]
46. Lutz MB, et al. An advanced culture method for generating large quantities of highly pure dendritic cells from mouse bone marrow. J Immunol Methods. 1999; 223:77–92. [PubMed: 10037236]
47. Siracusa MC, et al. TSLP promotes interleukin-3-independent basophil haematopoiesis and type 2 inflammation. Nature. 2011; 477:229–233. [PubMed: 21841801]

48. Kajiwara N, et al. Activation of human mast cells through the platelet-activating factor receptor. J Allergy Clin Immunol. 2010; 125:1137–1145. [PubMed: 20392487]

49. Tanaka S, et al. Expression of l-histidine decarboxylase in granules of elicited mouse polymorphonuclear leukocytes. Eur J Immunol. 2004; 34:1472–1482. [PubMed: 15114681]

50. Gerena RL, Eguchi N, Urade Y, Killian GJ. Stage and region-specific localization of lipocalin-type prostaglandin D synthase in the adult murine testis and epididymis. J Androl. 2000; 21:848–854. [PubMed: 11105911]

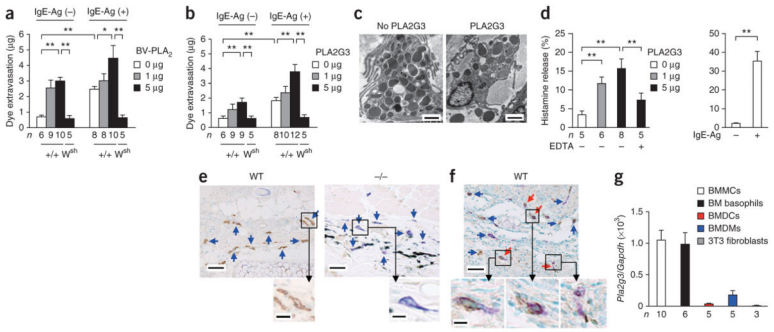

Figure 1.

PLA2G3 is expressed in mast cells and has the ability to induce degranulation. (**a**,**b**) Quantification of ear edema in IgE-sensitized *Kit*$^{+/+}$ (+/+) or *Kit*$^{W\text{-}sh/W\text{-}sh}$ (W^{sh}) mice 30 min after intradermal injection with 0 μg, 1 μg or 5 μg of BV-PLA$_2$ (**a**) or human PLA2G3 (**b**) in the presence (IgE-Ag (+)) or absence (IgE-Ag (−)) of 20 ng of antigen. (**c**) Transmission electron microscopy of ear mast cells in wild-type mice with (+) or without (−) administration of 5 μg of PLA2G3. Scale bars, 2 μm. (**d**) Histamine release from wild-type mouse peritoneal cells after treatment for 30 min with 0 μg, 1 μg or 5 μg of PLA2G3 in the presence or absence of 2 mM EDTA (left). Histamine release by IgE-Ag stimulation (positive control) is also shown (right). (**e**,**f**) Immunohistochemistry analysis of ear-skin sections of wild-type (WT) or *Pla2g3*$^{-/-}$ (−/−) mice before (**e**) and 2 min after (**f**) stimulation with IgE-Ag with anti-PLA2G3 (α-PLA2G3), followed by counterstaining with toluidine blue (scale bars, 50 μm). Boxed areas are magnified below (scale bars, 5 μm). Blue and red arrows indicate resting and degranulated mast cells, respectively. (**g**) Real-time PCR of *Pla2g3* relative to *Gapdh* in indicated bone marrow–derived cells from wild-type mice and Swiss 3T3 fibroblasts. Data are from one experiment (**g**), and compiled from two (**d**) and three (**a**,**b**) experiments (mean ± s.e.m.; **P* < 0.05 and ***P* < 0.01). Data in **c**,**e**,**f** are representative of two experiments.

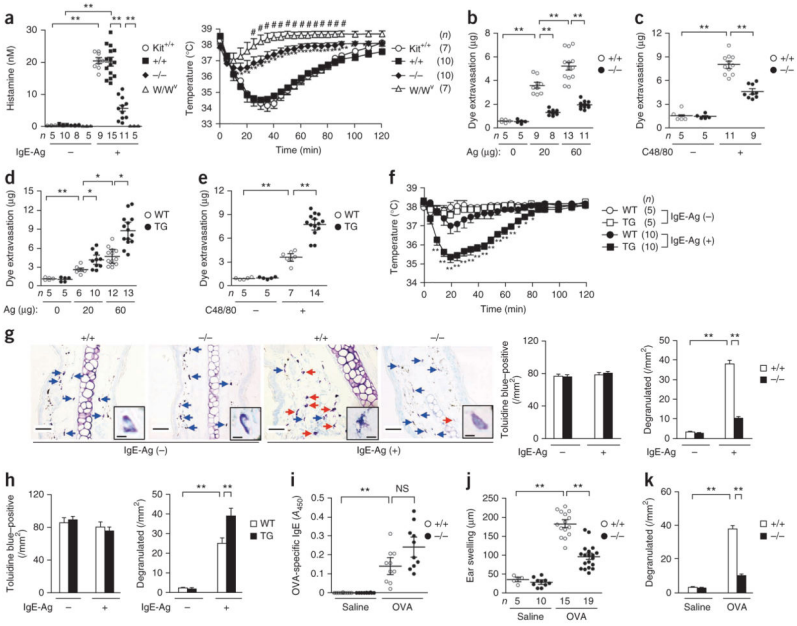

Figure 2.

Altered anaphylaxis in mice with deletion or overexpression of PLA2G3. (**a**) Serum histamine concentrations (left) and rectal temperatures (right) in IgE-Ag–dependent PSA in *Pla2g3*$^{+/+}$ (+/+), *Pla2g3*$^{-/-}$ (−/−), WBB6F1-*Kit*$^{+/+}$ (Kit$^{+/+}$) and WBB6F1-*Kit*$^{W/W\text{-}v}$ (W/W^{v}) mice after challenge with 500 μg of antigen (Ag). **P* < 0.05 and ***P* < 0.01, *Pla2g3*$^{-/-}$ versus *Pla2g3*$^{+/+}$ mice and $^{\#}P$ < 0.05, *Kit*$^{W/W\text{-}v}$ versus *Pla2g3*$^{-/-}$ mice (right). (**b**–**e**) Analysis of ear edema in IgE-Ag–induced (**b**,**d**) or C48/80–induced (**c**,**e**) PCA in *Pla2g3*$^{+/+}$ (+/+) and *Pla2g3*$^{-/-}$ (−/−) mice (**b**,**c**) or wild-type (WT) and *PLA2G3*$^{tg/+}$ (TG) mice (**d**,**e**). (**f**) Rectal temperatures in IgE-Ag–dependent PSA in wild-type (WT) and *PLA2G3*$^{tg/+}$ (TG) mice after challenge with antigen (25 μg). **P* < 0.05 and ***P* < 0.01, WT versus TG after antigen challenge. (**g**,**h**) Toluidine blue staining of skin sections (left) and counts of toluidine blue^{+} total and degranulated dermal mast cells (right) in *Pla2g3*$^{+/+}$ (+/+) and *Pla2g3*$^{-/-}$ (−/−) mice (**g**) or wild-type (WT) and *PLA2G3*$^{tg/+}$ (TG) mice (**h**) before (IgE-Ag (−)) and 2 min after (IgE-Ag (+)) IgE-Ag–mediated PCA (scale bars, 50 μm) (*n* = 6). Blue and red arrows indicate resting and degranulated mast cells, respectively (**g**). Insets, magnified images (scale bars, 5 μm) (**g**). (**i**–**k**) Serum levels of OVA-specific IgE (*n* = 10; **i**), ear swelling (**j**) and numbers of degranulated ear mast cells (*n* = 6; **k**) in OVA-induced active cutaneous anaphylaxis in *Pla2g3*$^{+/+}$ (+/+) and *Pla2g3*$^{-/-}$ (−/−) mice. Data are from one experiment (**f**–**i**,**k**) and compiled from three experiments (**a**–**e**,**j**) (mean ± s.e.m., **P* < 0.05; ***P* < 0.01; NS, not significant).

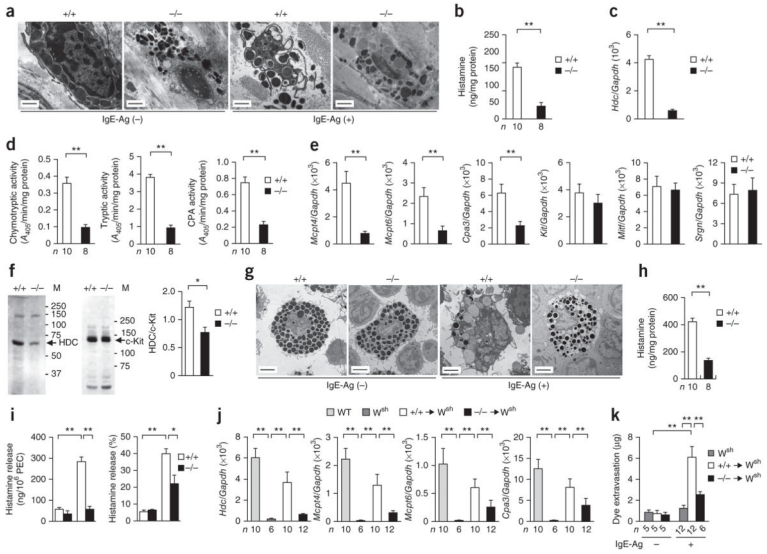

Figure 3.

Immature properties of tissue mast cells in *Pla2g3*-deficient mice. (**a**) Transmission electron micrographs of ear mast cells in *Pla2g3*$^{+/+}$ (+/+) and *Pla2g3*$^{-/-}$ (−/−) mice before (IgE-Ag (−)) and 2 min after (IgE-Ag (+)) antigen (Ag) challenge. Scale bars, 2 μm. (**b**,**c**) Quantification of histamine amounts (**b**) and *Hdc* mRNA expression relative to that of *Gapdh* (*n* = 12; **c**) in ears of *Pla2g3*$^{+/+}$ (+/+) and *Pla2g3*$^{-/-}$ (−/−) mice. (**d**,**e**) Quantification of protease activity (**d**) and mRNA expression of mast cell proteases (*n* = 12) and other mast-cell markers (*n* = 7) (**e**) in ears of *Pla2g3*$^{+/+}$ (+/+) and *Pla2g3*$^{-/-}$ (−/−) mice. (**f**) Immunoblotting of HDC and c-Kit in ears of *Pla2g3*$^{+/+}$ (+/+) and *Pla2g3*$^{-/-}$ (−/−) mice. M, molecular mass (kDa). The ratio of HDC/c-Kit was quantified by densitometric analysis (*n* = 4). (**g**) Transmission electron micrographs of pMCs in *Pla2g3*$^{+/+}$ (+/+) and *Pla2g3*$^{-/-}$ (−/−) mice before (IgE-Ag (−)) and 2 min after (IgE-Ag (+)) stimulation with antigen. Scale bars, 2 μm. (**h**,**i**) Quantification of histamine content (**h**) and IgE-Ag–induced histamine release (quantity and percentage; **i**) in *Pla2g3*$^{+/+}$ (+/+) and *Pla2g3*$^{-/-}$ (−/−) pMCs. PEC, peritoneal cells. (**j**,**k**) Expression of mast-cell marker mRNAs (**j**) and dye extravasation in IgE-Ag–dependent PCA (**k**) in ears of *Pla2g3*$^{+/+}$ (+/+) or *Pla2g3*$^{-/-}$ (−/−) BMMC-reconstituted or nonreconstituted *Kit*$^{W\text{-}sh/W\text{-}sh}$ (W^{sh}) mice and wild-type (WT) *Kit*$^{+/+}$ mice. Data are compiled from two (**d**,**h**,**i**) or three (**b**,**c**,**e**,**j**,**k**) experiments (mean ± s.e.m., **P* < 0.05; ***P* < 0.01). Images are representative of one (**f**) or two (**a**,**g**) experiments.

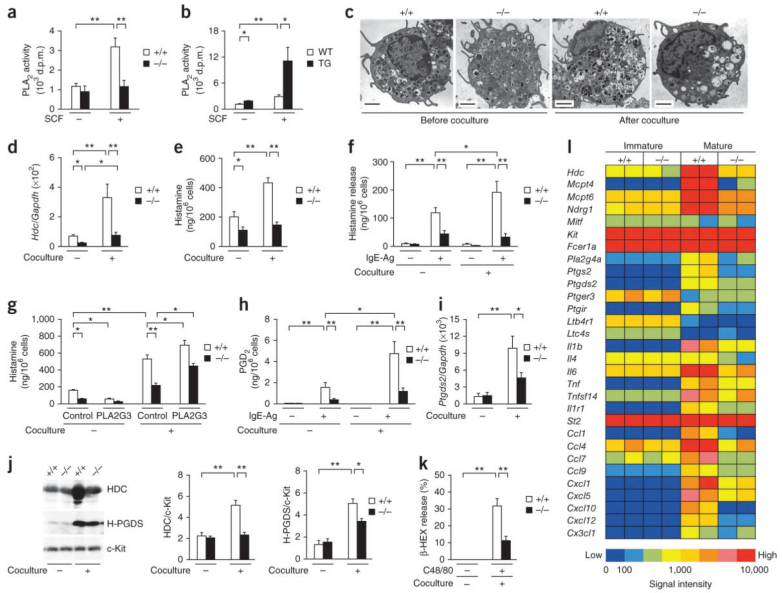

Figure 4.

Defective fibroblast-driven maturation of *Pla2g3*$^{-/-}$ BMMCs. (**a**,**b**) Release of sPLA$_2$ activity from *Pla2g3*$^{+/+}$ (+/+) and *Pla2g3*$^{-/-}$ (−/−) BMMCs (**a**) or from *PLA2G3*$^{tg/+}$ (TG) and wild-type (WT) BMMCs (**b**) with or without 100 ng/ml SCF for 30 min (n = 4). d.p.m., disintegrations per minute. (**c**) Transmission electron microscopy of *Pla2g3*$^{+/+}$ (+/+) and *Pla2g3*$^{-/-}$ (−/−) BMMCs before and on day 4 of coculture with Swiss 3T3 fibroblasts. Scale bars, 2 μm. (**d**–**k**) Expression of *Hdc* relative to *Gapdh* (n = 8; **d**), cellular histamine levels (n = 8; **e**), histamine release with (IgE-Ag (+)) or without (IgE-Ag (−)) antigen challenge (n = 8; **f**), cellular histamine levels after culture in the presence or absence (control) of 2 μg/ml human PLA2G3 (n = 6; **g**), PGD$_2$ generation with or without antigen challenge (n = 8; **h**), *Ptgds2* expression (n = 8; **i**), immunoblot of HDC (n = 6) and H-PGDS (n = 3) relative to c-Kit (**j**) and C48/80-induced β-HEX release (n = 7; **k**) in *Pla2g3*$^{+/+}$ (+/+) or *Pla2g3*$^{-/-}$ (−/−) BMMCs before (−) and on day 4 of (+) coculture. (**l**) Microarray gene profile of *Pla2g3*$^{+/+}$ (+/+) and *Pla2g3*$^{-/-}$ (−/−) BMMCs before immature and on day 4 of mature coculture. Results from duplicate experiments are shown (columns). Heat maps are globally normalized for all genes. Data are from one experiment (**a**,**b**,**l**) and compiled from two (**d**,**e**,**g**,**j**,**k**) or three (**f**,**h**,**i**) experiments (mean ± s.e.m., *P < 0.05; **P < 0.01). Images in **c** are representative of two experiments.

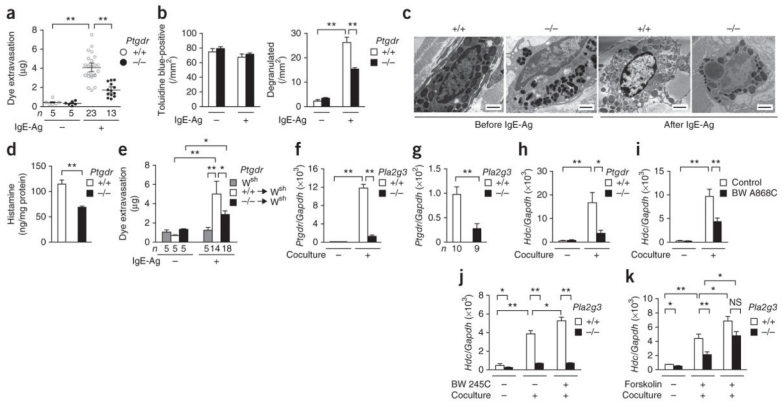

Figure 5.

Defective mast-cell maturation and anaphylaxis by DP1 deficiency. (**a**) Quantification of ear edema in PCA in *Ptgdr*$^{+/+}$ (+/+) and *Ptgdr*$^{-/-}$ (−/−) mice with (IgE-Ag (+)) or without (IgE-Ag (−)) antigen challenge. (**b**) Counts of toluidine blue^{+} dermal mast cells in *Ptgdr*$^{+/+}$ (+/+) and *Ptgdr*$^{-/-}$ (−/−) mice before and 2 min after IgE-Ag–mediated PCA (n = 6). Number of degranulated mast cells were evaluated by staining of skin sections from *Ptgdr*$^{+/+}$ and *Ptgdr*$^{-/-}$mice with toluidine blue, as in Figure 2g. (**c**) Transmission electron microscopy of ear mast cells in *Ptgdr*$^{+/+}$ (+/+) and *Ptgdr*$^{-/-}$ (−/−) before (IgE-Ag (−)) and 2 min after (IgE-Ag (+)) antigen challenge. Scale bars, 2 μm. (**d**) Histamine levels in ears of *Ptgdr*$^{+/+}$ and *Ptgdr*$^{-/-}$ mice (n = 10). (**e**) Quantification of ear edema in IgE-Ag–dependent PCA in *Kit*$^{W\text{-}sh/W\text{-}sh}$ (W^{sh}) mice with or without reconstitution with *Ptgdr*$^{+/+}$ (+/+) or *Ptgdr*$^{-/-}$ (−/−) BMMCs. (**f**,**g**) Expression of *Ptgdr* in *Pla2g3*$^{+/+}$ and *Pla2g3*$^{-/-}$ BMMCs before and on day 2 of coculture (n = 6; **f**) and in the ear of *Pla2g3*$^{+/+}$ and *Pla2g3*$^{-/-}$ mice (**g**). (**h**,**i**) Expression of *Hdc* relative to *Gapdh* in *Ptgdr*$^{+/+}$ and *Ptgdr*$^{-/-}$ BMMCs (n = 6; **h**) or in wild-type BMMCs with or without BW A868C (n = 7; **i**) before and on day 2 of coculture. (**j**,**k**) Expression of *Hdc* relative to *Gapdh* in *Pla2g3*$^{+/+}$ and *Pla2g3*$^{-/-}$ BMMCs before and on day 2 of coculture with or without BW 245C (n = 6; **j**) or forskolin (n = 6; **k**). Data are compiled from two (**b**,**d**,**f–k**) or three (**a**,**e**) experiments (mean ± s.e.m., *P < 0.05; **P < 0.01; NS, not significant). Images in **c** are representative of two experiments.

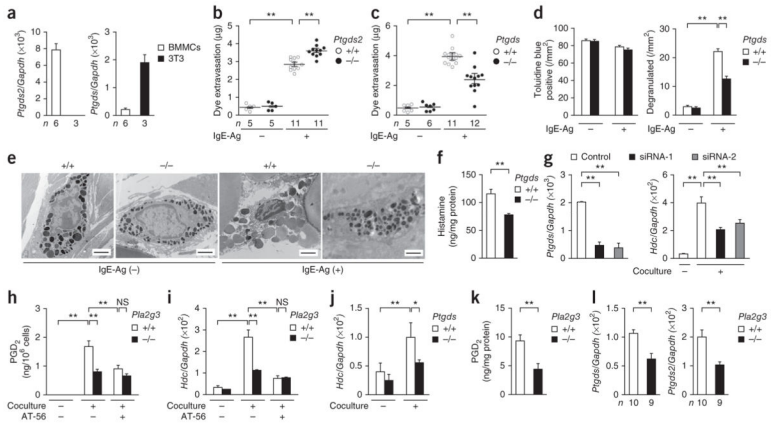

Figure 6.

Defective mast-cell maturation and anaphylaxis by L-PGDS deficiency. (**a**) Expression of *Ptgds* and *Ptgds2* relative to *Gapdh* in wild-type BMMCs and Swiss 3T3 fibroblasts. (**b**,**c**) Quantification of ear edema in PCA in *Ptgds*$^{-/-}$ (**b**), *Ptgds2*$^{-/-}$ (**c**) mice (−/−) and littermate wild-type (+/+) mice with (IgE-Ag (+)) or without (IgE-Ag (−)) antigen challenge. (**d**) Dermal mast-cell counts in *Ptgds*$^{+/+}$ and *Ptgds*$^{-/-}$ mice before and 2 min after IgE-Ag–mediated PCA (n = 6). Number of degranulated mast cells were evaluated by staining of skin sections with toluidine blue, as in Figure 2g. (**e**) Transmission electron microscopy of *Ptgds*$^{+/+}$ (+/+) and *Ptgds*$^{-/-}$ (−/−) ear mast cells before (IgE-Ag (−)) and 2 min after (IgE-Ag (+)) antigen challenge. Scale bars, 2 μm. (**f**) Histamine levels in ears of *Ptgds*$^{+/+}$ and *Ptgds*$^{-/-}$ mice (n = 10). (**g**) *Ptgds* expression in Swiss 3T3 fibroblasts after *Ptgds* or scrambled siRNA treatment and *Hdc* expression in wild-type BMMCs before and on day 2 of coculture with siRNA-treated fibroblasts (n = 7). (**h**,**i**) PGD_2 generation (**h**) and *Hdc* expression (**i**) before and on day 1 of coculture of *Pla2g3*$^{+/+}$ or *Pla2g3*$^{-/-}$ BMMCs with Swiss 3T3 fibroblasts with or without AT-56 (n = 6). (**j**) *Hdc* expression in wild-type BMMCs before and on day 4 of coculture with *Ptgds*$^{+/+}$ (+/+) or *Ptgds*$^{-/-}$ (−/−) skin fibroblasts (n = 6). (**k**,**l**) PGD_2 levels (n = 10; **k**) and *Ptgds* and *Ptgds2* expression (**l**) in the ear skin of *Pla2g3*$^{+/+}$ and *Pla2g3*$^{-/-}$ mice. Data are compiled from two (**a**,**d**,**f**,**h**–**l**) or three (**b**,**c**,**g**) experiments (mean ± s.e.m., *P < 0.05; **P < 0.01; NS, not significant). Images in **e** are representative of two experiments.

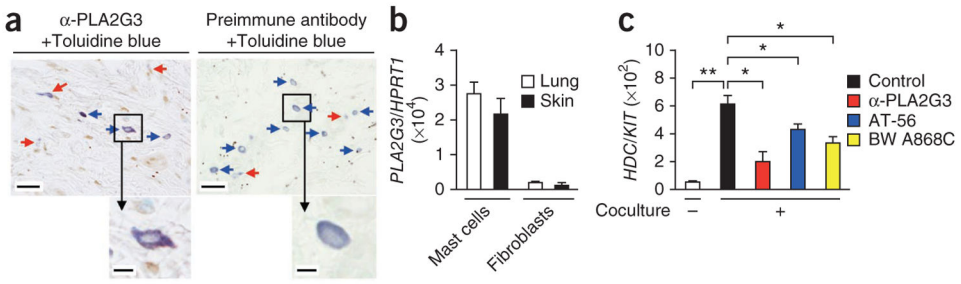

Figure 7.

The PLA2G3–L-PGDS–DP1 axis facilitates maturation of human mast cells. (**a**) Immunohistochemistry analysis of human skin sections (atopic dermatitis) with anti-PLA2G3 (α-PLA2G3) or a preimmune antibody, followed by counterstaining with toluidine blue (scale bars, 50 μm). Blue and red arrows indicate resting and degranulated mast cells, respectively. Boxed areas are magnified below (scale bars, 5 μm). (**b**) Expression of *PLA2G3* relative to *HRPT1* in primary mast cells and fibroblasts obtained from human skin and lung ($n = 3$). (**c**) Expression of *HDC* relative to *KIT* in human lung mast cells before or on day 4 of coculture with human lung fibroblasts in the presence or absence of 5 μg/ml anti-PLA2G3, 10 μM AT-56 or 1 μM BW A868C ($n = 4$). Data are from one experiment (**b**,**c**; mean ± s.e.m., $*P < 0.05$; $**P < 0.01$). Images in **a** are representative of two experiments.